CrossMark

The effect of number of SILAR cycles on morphological, optical and photo catalytic properties of cadmium sulfide–titania films

M. M. Momeni[1] · A. A. Mozafari[1]

Abstract In this paper, cadmium sulfide–titania nanocomposites were successfully synthesized by electrochemical anodizing and successive ionic layer adsorption and reaction (SILAR) methods. Cadmium sulfide was successfully deposited on titania nanotubes with tunable loading amounts by controlling deposition cycles of SILAR. The morphology, crystal structure, elemental composition and light absorption capability of samples were characterized by FE-SEM, XRD, EDX and UV–Vis methods. Titania nanotubes with 90–220 nm in diameter and 15–30 nm in wall thickness were prepared by one-step anodizing method and then cadmium sulfide deposited onto titania to form cadmium sulfide–titania heterostructure. Characterization of the cadmium sulfide–titania sample indicated that the number of SILAR cycles significantly influenced the morphology and photo catalytic activity of fabricated films. Rh B and MO were adopted as the model dyes and the photo catalytic tests were carried out in detail. Results showed that the photo catalytic activity of cadmium sulfide–titania samples is higher than that with bare titania sample. The incorporation of cadmium sulfide on titania improves the photo catalytic activity due to the synergetic effect. The photo catalytic activity increase with the proper increase of cadmium sulfide amount; however, the activity decreases when the amount of cadmium sulfide is further increased which may result in the formation of the compact films on the surface and a decrease in surface area of samples. Cadmium sulfide–titania sample prepared by SILAR deposition with 5 cycles gives the highest degrading rate, which can be attributed to appropriate cadmium sulfide content. Cadmium sulfide–titania is easy to be recycled and has good stability for repeated use. A mechanism is also studied and an electron transfer route is provided and accounts for the enhanced photo catalytic activity. With the improved visible light degradation performance, cadmium sulfide–titania samples would be expected to be used in water purification.

1 Introduction

Titania nanotubes have attracted much attention due to their unique structural and electronic properties and have various applications in a lot of fields, such as solar cells, lithium batteries, photo-detectors, light waveguides, gas sensing and photo catalysis [1–4]. These one-dimensional nanostructured possess high specific surface area and nanotubular morphology, the nanotubular features of titania provide a large amount of channels for enhanced electron transfer, which is important during photo catalytic oxidation of organic compounds [1–4]. However, titania nanotubes have the intrinsic drawbacks of poor visible-light absorption (wide band gap semiconductor which can only absorb UV light with the wavelength below 390 nm) and fast charge carrier recombination (photo-generated electrons and holes) which hinder its practical application [5]. Many strategies have recently been devoted to modify titania nanotubes by dye sensitization, doping with ions, coating their surface with noble metal nanoparticles or narrow band-gap semiconductor quantum dots and coupling with low band gap semiconductors like PbS, CdTe, CdSe, $ZnFe_2O_4$, Cu_2O, CdS; which may overcome the

✉ M. M. Momeni
momeni22@gmail.com

✉ A. A. Mozafari
a.mozafari@ch.iut.ac.ir

[1] Department of Chemistry, Isfahan University of Technology, Isfahan 84156-83111, Iran

above defects and improve the catalytic efficiency [6–22]. Among the low band gap semiconductors, cadmium sulfide (CdS) has attracted much attention; it can be excited by visible light to produce electrons and holes due to the narrow band gap of 2.4 eV [22, 23]. Cadmium sulfide was often deposited or coated on nanorod arrays of zinc oxide and titanium dioxide, which were used as high surface area templates to enhance solar absorption and as semiconductors to form a junction with cadmium sulfide [24–34]. Previous studies have shown that in the cadmium sulfide/ titania system, heterojunctions between titania and CdS are formed and the conduction band (CB) of cadmium sulfide is about 0.5 eV (more negative than that of titania). So no holes generated in the CB of titania, and the recombination of electrons–holes pairs is inhibited in the cadmium sulfide/ titania system. As a result, the coupled system can enhance light-harvesting efficiency, thus improving the photo catalytic performance of the catalyst [22]. In the present study, hybrid cadmium sulfide–titania nanostructures were prepared by using of electrochemical anodizing and successive ionic layer adsorption and reaction (SILAR) methods. The morphology and structure were characterized by scanning electron microscopy, energy dispersive X-ray spectroscopy and X-ray diffraction. Optical properties were investigated by UV–visible diffuse reflectance spectra. In addition, photo catalytic activity of different hybrid cadmium sulfide–titania nanostructure samples was investigated and compared by degradation of some dyes. Results show that the presence of cadmium sulfide significantly improved the photo catalytic performance of samples.

2 Experimental

All chemicals were obtained as analytical reagent grade and used without further purification. The solutions were prepared with distilled water. Titanium foils (purity >99.99 %, 1 mm thickness) were used.

Titanium plates were cut into desired dimensions and were employed as substrate for the preparation of the titania nanotubes/Ti working electrode with only one face exposed to solution. They were mechanically polished with different abrasive papers (with the following grades: 80,180, 400, 600, 1200 and 2000), rinsed in a bath of distilled water, then chemically etched by immersion in a HF/HNO$_3$/H$_2$O (1:4:5 in volume) mixed solution, and finally rinsed with distilled water. They were then dried in air at room temperature. Pretreatment by this procedure ensures a good adhesion of the deposit to the substrate. After cleaning, anodic films were grown from titanium by anodizing of this foil in a solution of ethylene glycol (98 mL) containing 0.13 M NH$_4$F and 2 mL distilled water

at a constant voltage of 60 V for 6 h at room temperature using a graphite foil with about 12 cm^2 geometric areas as cathode. Anodizing was carried out using a controlled DC power supply source (ADAK, PS405). A schematic representation of the anodizing setup is shown in Fig. 1. After anodizing, the as-formed samples were annealed in air atmosphere at 400 °C for 2 h with a ramp of 2 °C/min to obtain crystalline samples.

Cadmium sulfide was deposited on the titania nanotubes by separately SILAR method. Titania nanotubes were dipped into 0.5 M Cd(NO$_3$)$_2$ in ethanol for 10 min, rinsed with ethanol, dried in air, dipped for another 10 min into a 0.5 M Na$_2$S aqueous solution and rinsed again with distilled water and dried at 150 °C for 10 min, which was defined as one SILAR cycle. The deposition of CdS was repeated for 6 cycles. In order to investigate the influence of deposition conditions on samples property, we changed the deposition cycle (1, 2, 3, 4, 5 and 6 cycles) into carry out the CdS/TiO$_2$ samples (CdST). The as prepared samples were named respectively CdST-1, CdST-2, CdST-3, CdST-4, CdST-5 and CdST-6, that terminal number is the number of SILAR cycles.

The surface morphology of all samples was characterized by field emission scanning electron microscopy (FE-SEM, Hitachi S-4160, Japan), and the elemental composition was estimated by energy dispersive X-ray spectroscopy (EDX). Elemental mapping was conducted by energy dispersive spectroscopy (EDS). The crystalline phases were identified by XRD (Philips X'Pert). Diffraction patterns were recorded in the 2θ range from 20° to 80° at room temperature. The optical absorption of the samples was determined using a diffuse reflectance UV–visible spectrophotometer (JASCO V-570).

Photo catalytic activities of all the samples were evaluated by degradation of rhodamine B (Rh B) and methyl orange (MO) under visible light irradiation. The photo catalytic reaction was carried in a single-compartment cylindrical quartz reactor. A 200 W xenon lamp accompanied with a UV cutoff filter was used as a light source to provide visible light. The luminous intensity of the xenon lamp was 100 mW Cm^{-2}. The actual experiments were performed at room temperature. Prior to illumination, the photo catalyst sample was immersed in quartz reactor containing Rh B or MO, magnetically stirred for 120 min in the dark to ensure the establishment of an adsorption–desorption equilibrium between the photo catalyst and these dyes. Then the solution was exposed to visible light irradiation under magnetic stirring. At certain time intervals, specific amount of the solution was withdrawn and the changes in concentration of dye were observed using a UV–Vis spectrophotometer. The maximum absorption wavelengths of MO and Rh B are 462 and 554 nm, respectively.

Fig. 1 Schematic presentation of the pretreatment method of titanium sheets and producing process of TiO$_2$ nanotube films on titanium foils
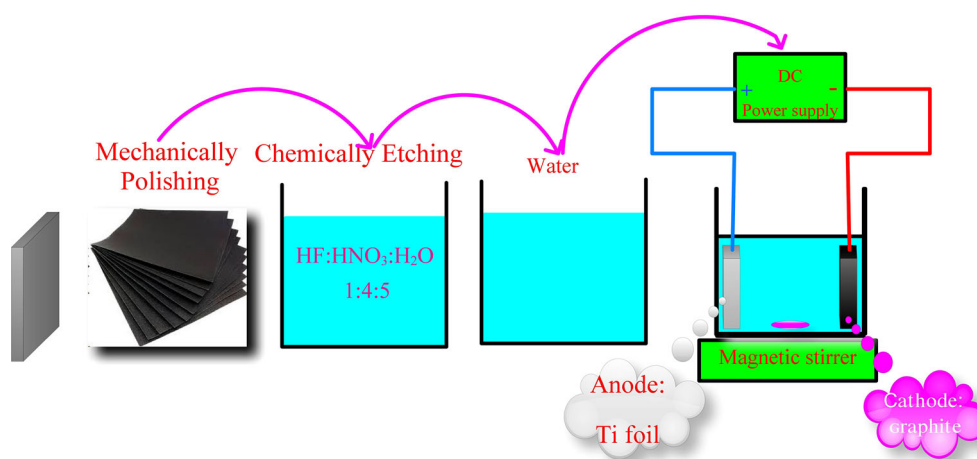
3 Results and discussion

The SILAR method, introduced by Nicolau, is a unique method in which thin films of compound semiconductors can be deposited by alternate dipping of a substrate into the aqueous solutions containing ions of each component. The SILAR technique is a solution phase method to grow thin films at room temperature and ambient pressure. The SILAR method resembles CBD but deposition control of the growth is easier since the precursors for the cation and anion constituents of the thin film are in different vessels. The growth of thin films in the SILAR method occurs only heterogeneously on the solid–solution interface due to the intermediate rinsing step between the cation and anion immersions. Therefore, the thickness of the film can be controlled simply by the number of growth cycles. Between each precursor treatment, the surface is rinsed with purified water or ethanol so that only the tightly adsorbed layer stays on the substrate. Hence, the reaction producing a thin film occurs only on the surface of the substrate. The equipment for the SILAR technique can be very simple and inexpensive due to the ambient growth conditions used [35, 36]. In SILAR method, the growth mechanism involves three most important steps:

1. Specific adsorption of the most strongly adsorbed ions of the compound to be grown by substrate immersion in a solution of one of its salts
2. Water or ethanol rinsing of the excess solution still adhering to the substrate
3. Chemical reaction between the most strongly specifically adsorbed ions and the less strongly adsorbed ones by the subsequent substrate immersion in a solution containing the latter, entailing the growth.

The schematic diagram of a single SILAR cycle for CdS deposited on TiO$_2$ nanotubes is presented in Fig. 2.

The morphology of prepared samples were observed by SEM. Figure 3a shows FE-SEM images of bare titania sample, which clearly shows formation of nanotube–nonoporous films on the surface of titanium that the surface of them was open. It can be seen that their diameter is in the range of 90–220 nm and wall thickness of 15–30 nm. The FE-SEM of the as-prepared cadmium sulfide–titania samples was illustrated in Fig. 3b–g. In Fig. 3b–f, cadmium sulfide–titania samples displayed nonoporous that the surface of them was open. By increasing the cycle number of SILAR, more amounts of cadmium sulfide have been deposited on the surface. In Fig. 3g, nanostructure films can not be seen on the surface. Compact films, without porosity, were formed on the surface of samples. It can be said that when the number of SILAR cycles increased to 6 cycles, surface is covered with a compact layer of cadmium sulfide.

The analysis of the films surface by energy dispersive X-ray spectroscopy (EDX) taking measurements on top and results present in Fig. 4. It was seen that the films mainly consisted of Ti, O, Cd and S; the contents of each sample were inserted in the corresponding figure. The EDX data of cadmium sulfide–titania samples show two peaks around 4.5 and 4.9 keV for Ti. The peaks due to cadmium are clearly distinct at 0.4, 3.1 and 3.3 keV. Also peaks due to sulfur were appeared at 0.1 and 2.3 keV. These results confirm that Ti, O, Cd and S exist in these samples. The occurrences of traces of contaminants such as N, F and Na from precursors are also observed. The composition of the cadmium sulfide–titania sample was confirmed by energy-dispersive X-ray mapping (Fig. 5). This test shows the presence of Cd, O, Ti, S, Na, F and N in these samples. The elemental maps demonstrated that O, Ti, Cd and S are homogeneously distributed on the surface of samples.

The phase structures of samples were determined by X-ray diffraction (XRD). The XRD patterns of the bare

Fig. 2 Schematic presentation of single SILAR cycle for CdS deposited on TiO_2 and preparation of CdS/TiO_2 nanocomposite electrodes
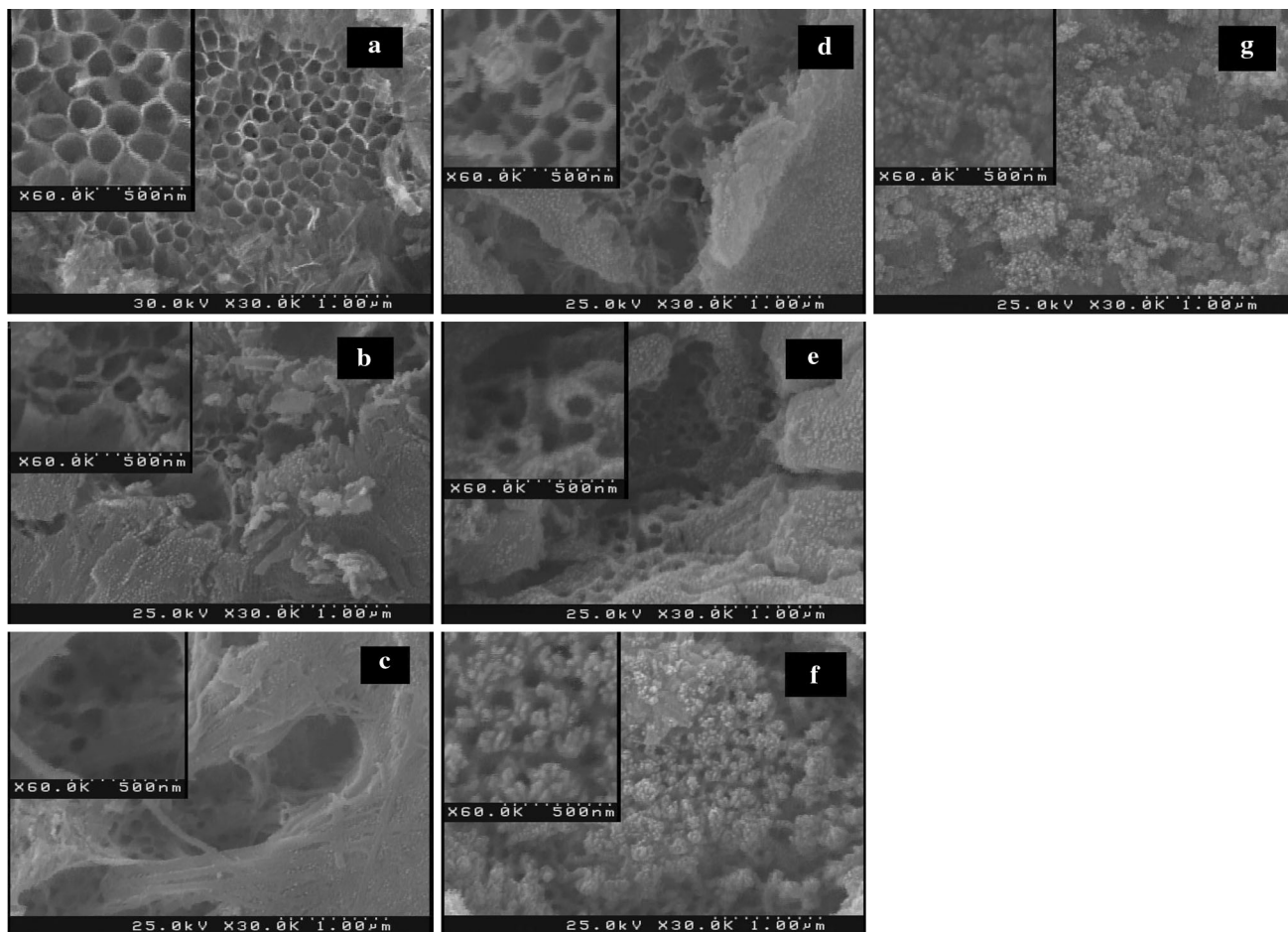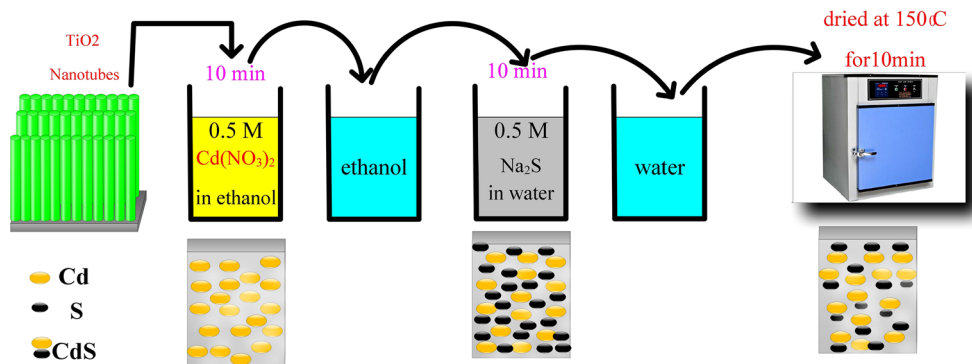

Fig. 3 a SEM top-view image of different samples; **a** as-prepared TiO_2 nanotubes; **b** CdST-1, **c** CdST-2, **d** CdST-3, **e** CdST-4, **f** CdST-5 and **g** CdST-6

titania and cadmium sulfide–titania samples are shown in Fig. 6. Figure 6 shows XRD patterns of (a) as-prepared bare titania, (b) bare titania annealed at 400 °C and (c) cadmium sulfide–titania samples. Diffractions that are attributable to anatase TiO_2 are clearly observed in the annealed sample. The Ti peaks were due to the titanium substrate. As shown in this figure, the peaks at $2\theta = 25.3°$, 37.9°, 38.6°, 54.0°, 55.2°, 62.9°, 75.3° and 76.2° were

assigned to the TiO_2 anatase phase (JCPD card no. 01-073-1764). Comparing the XRD patterns of b and c show that apart from the existed diffraction peaks in b and c spectra which are related with the characteristic diffraction peaks of TiO_2, other specific diffraction peaks at 24.8°, 26.5°, 28.2°, 43.7°, 47.8°, 50.9°, 52.8°, 58.2° and 69.2° also appear in c spectrum. According to the standard PDF (JCPD card no. 01-075-1545) of CdS, the nine extra

Fig. 4 EDX spectrum of different samples; **a** CdST-2 and **b** CdST-6 sample
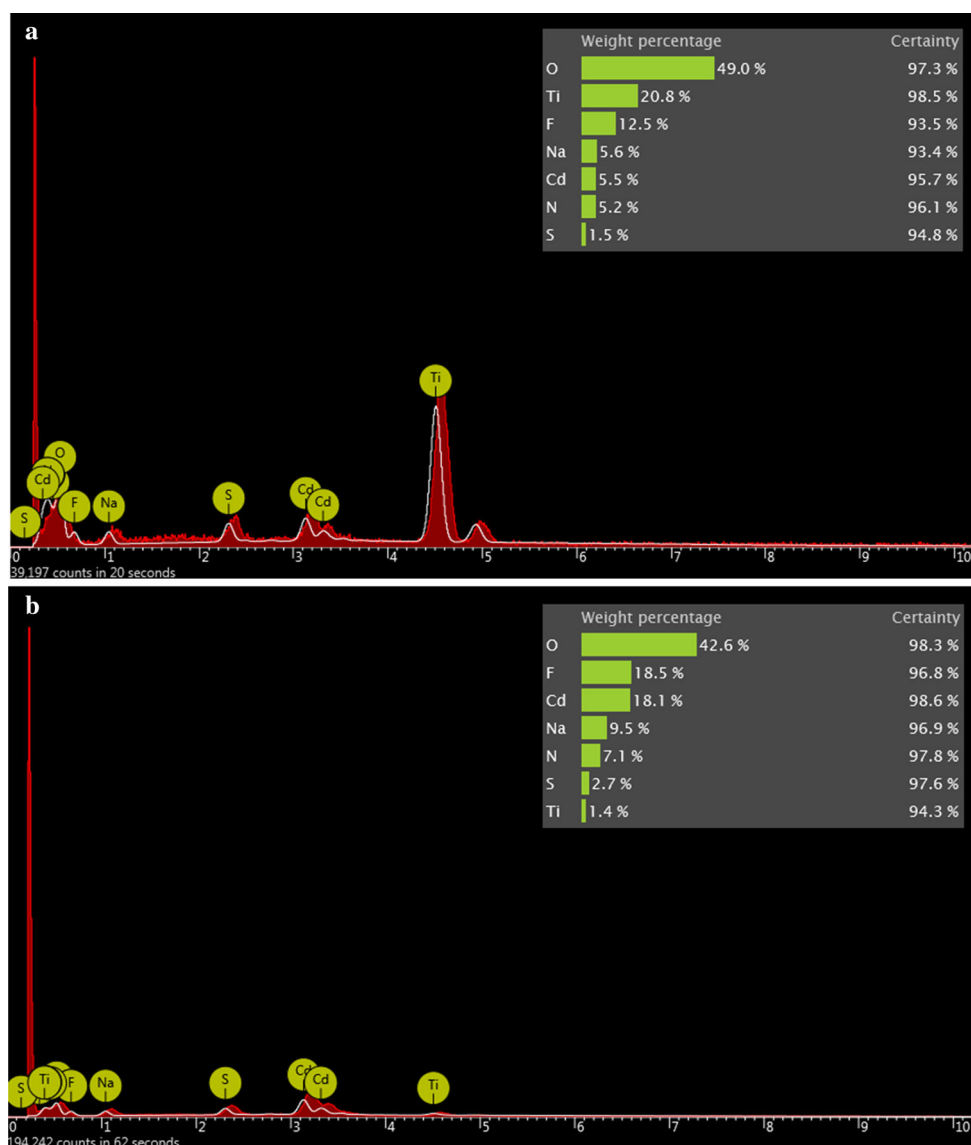
specific diffraction peaks in c spectrum correspond with (100), (002), (101), (110), (103), (200), (201), (202) and (210) of crystal planes of cadmium sulfide. The XRD data further confirms the successful preparation of cadmium sulfide–titania photo catalysts.

The band gap in a semiconductor material is closely related to the wavelength range absorbed, where the band gap decreases with increasing absorption wavelength. Consequently, a material with a narrow band gap can be extended readily to utilize visible light, whereas a narrow band gap can reduce photo catalytic activity by increasing the recombination rate between the electrons and holes. Figure 7 shows the UV–Vis absorption spectra of bare titania nanotube and different cadmium sulfide–titania samples prepared with different cycles of SILAR processes. An absorption in UV region (<400 nm) was observed for all the samples, which can be assigned to the

intrinsic band gap absorption of TiO_2. Compared with bare titania, cadmium sulfide–titania samples show the same absorption edge, indicating that cadmium sulfide was not incorporated into the lattice of TiO_2, but only deposited on its surface. Moreover, the absorption wavelength range of titania samples is extended greatly toward visible light, and the wide visible-light absorption becomes stronger with increasing cadmium sulfide content.

Photo catalytic activity of different samples was followed through degradation of rhodamine B and methyl orange as a function of irradiation time with visible light. To get the response of photo catalytic activities of bare titania and cadmium sulfide–titania samples, the absorption spectra of exposed samples at various time intervals were recorded and the rate of color degradation was observed in terms of change in intensity at λ_{max} of these dyes. In practice, the first, dyes degradation experiments were
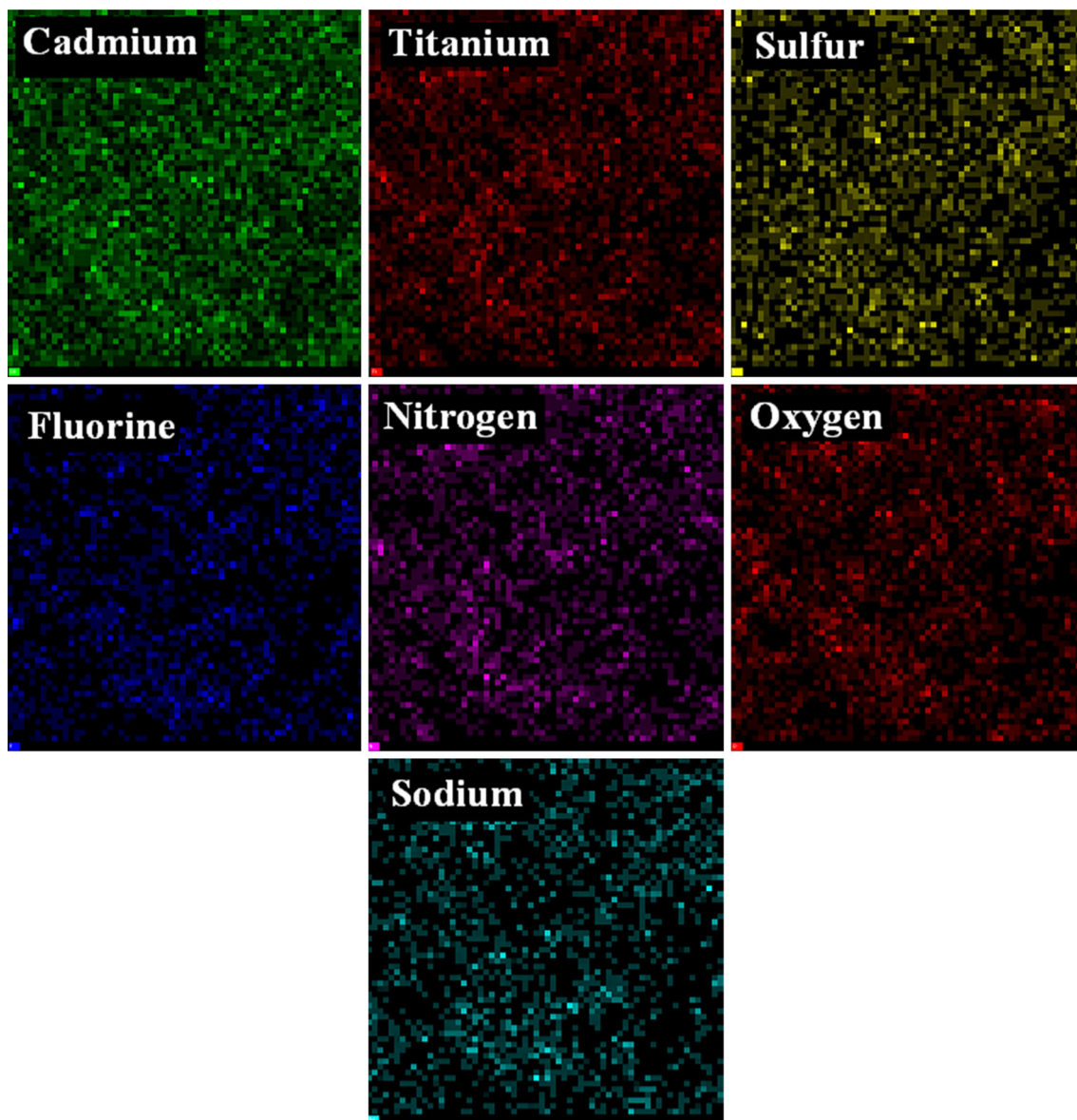
Fig. 5 Elemental EDX mapping of Ti, O, Cd and S obtained from CdST-6 sample

conducted under light irradiation to evaluate direct photolysis without the addition of any catalyst. The concentration of dyes remained nearly constant after irradiation. Thus, no obvious degradation of these dyes was observed in this time period. In addition, a dark control experiment was conducted, indicating that the adsorption of these dyes onto the surface of the catalyst in the absence of light radiation was negligible. The photo catalysis results indicated that the photo catalytic process was very effective in the removal of these dyes and it was observed that the degradation of dyes was enhanced using cadmium sulfide–titania samples.

Figure 8a shows the photo degradation rate of Rh B under visible light in presence of different samples.

the irradiation of visible light, bare titania (T) sample showed almost no photo catalytic activity, but cadmium sulfide–titania (CdST) samples showed photo catalytic activity. Figure 8a show that the CdST-5 sample exhibited better photo catalytic activity than other samples under visible light illumination. The photo catalytic performances of different samples were in the following order:

$$CdST\text{-}5 > CdST\text{-}4 > CdST\text{-}3 > CdST\text{-}2 > CdST1$$
$$> CdST\text{-}6 > T$$

Figure 8b shows the photo degradation rate of MO under visible light in presence of different samples. Because of its stabilization and low photosensitized property, MO solution was more difficult to be decolorized
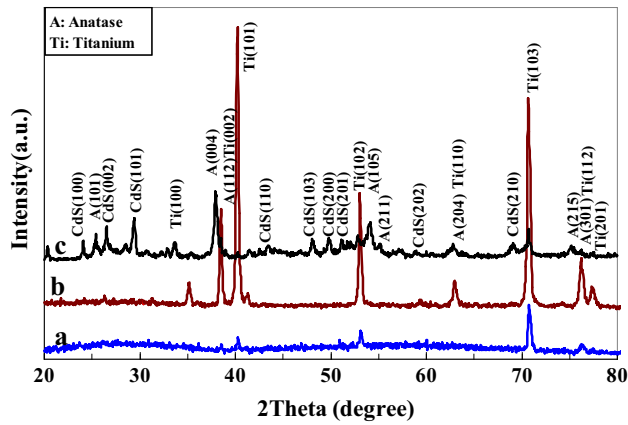
Fig. 6 XRD patterns of prepared samples, **a** as-prepared bare TiO₂, **b** bare TiO₂ annealed at 400 °C for 2 h and **c** CdST-6 sample
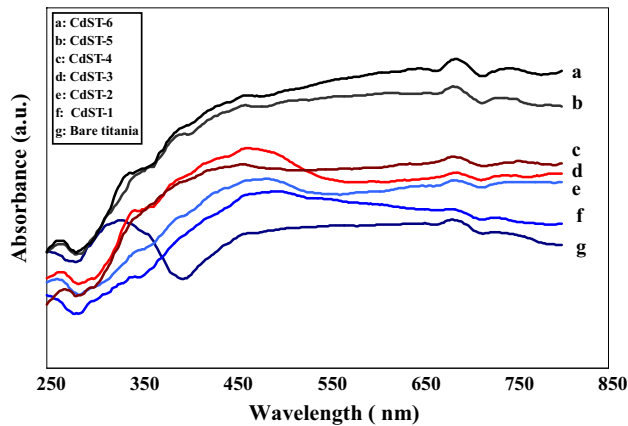

Fig. 7 Diffuse reflectance UV–Vis absorption spectra of different samples

compared to Rh B. However, as can be seen in Fig. 8b, CdST-5 presented highest photo catalytic activity under visible light irradiation among all samples, and the decoloration efficiency of MO solution was 91 % under visible light irradiation for 300 min. This further confirmed that CdST-5 exhibited excellent visible light photo catalytic activity. As can be seen, the decoloration of Rh B and MO over different samples shows similar trends: CdST-5 possess the highest photo catalytic activity under visible light irradiation among all the samples. The excellent crystallinity, the improvement of visible-light absorption (capability to absorb visible light and higher light absorption, compared to bare titania), larger surface area, the unique morphologies and nanostructures of cadmium sulfide–titania (CdST) samples, the intimate contact and the synergistic effect within the heterojunctions between cadmium sulfide and titania, were supposed to be responsible for the highly efficient photo catalytic activity of CdST.
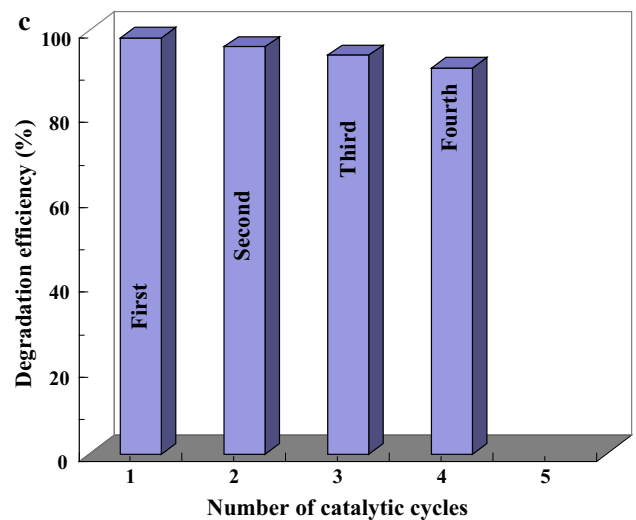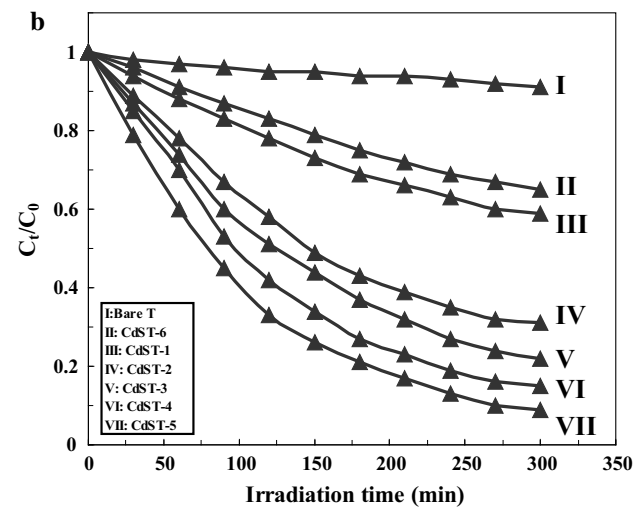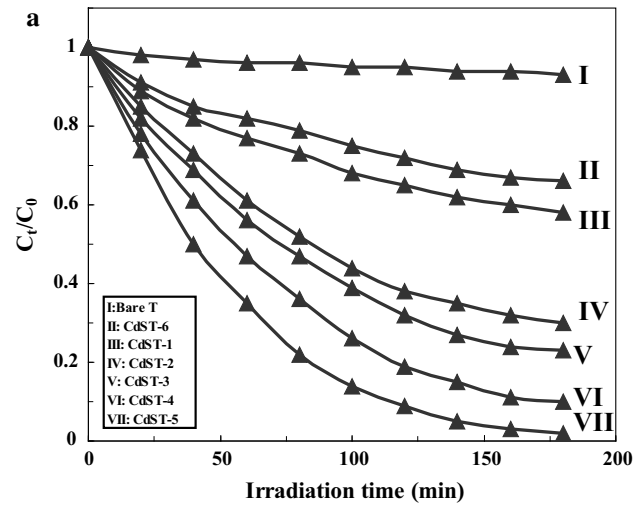

Fig. 8 The photo catalytic degradation of Rh B solution (**a**) and MO solution (**b**) by the different samples under visible light irradiation. **c** Photo catalyst stability test of prepared samples for degradation of MO solution

In addition to the photo catalytic activity, the stability of the photo catalysts is another important issue for practical application, for it can be regenerated and reused. To investigate the stability of prepared sample, four runs of cycling photo degradation experiments under identical conditions were performed (Fig. 8c). Before each experiment, the used photo catalyst was cleaned through washing with distilled water. Compared with the common catalysts in the powder form that nanoparticles dispersed in the reaction media, our samples prepared on the titanium substrates are more conveniently separated and recycled without any laborious centrifugation. As shown in Fig. 8c, after a 4-cycle experiment, this catalyst exhibited similar catalytic performance without significant deactivation, indicating its high durability and stability. Therefore, the recycling of CdST is possible, prepared samples in this study should be a promising photo catalyst for treatment of organic contamination

In here, a simple photo catalytic mechanism has been investigated. Figure 9 shows the schematic diagram of the separation of photo-generated electrons–holes pairs on the interface of CdS/TiO$_2$ under visible light irradiation. When the CdS/TiO$_2$ compound were irradiated by the visible light with a photon energy higher or equal to the band gaps of CdS (due to its narrow energy band gap that is ~ 2.4 eV), CdS is excited to yield electron–hole pairs under visible light irradiation and electrons in their valence band (VB) could be aroused to their corresponding conduction band (CB) with simultaneous generation of the same amount of holes in their VB [Eq. (1)]. Then, the photo-induced electrons and holes could be separated under the influence of the electrostatic field induced by the different work functions of the semiconductors their VB [22]. The photo-induced electron transfer would occur from the CB of CdS to the CB of TiO$_2$ (because of the

Fig. 9 Schematic diagram of charge transfer in CdS/TiO$_2$ photo catalyst for visible-light photo catalysis and proposed reaction mechanism

matched CB potential position and the intimate contact between CdS and TiO$_2$), whereas the photo-induced holes still remained in the VB of CdS, the photo-induced charge carriers in CdS could be effectively separated [Eq. (2)]. Such an interfacial charge transfer will bring down recombination of photo-generated charge carries. Therefore the above results we presume the hetero-structures do larger the absorption range to visible-light region. After stimulation of CdS under visible light irradiation and creating electron–hole pairs, in the next step, the electrons in the CB of TiO$_2$ react with molecular oxygen to generate superoxide radical ($^{\cdot}O_2{}^-$) [Eq. (3)] and hydrogen peroxide (H_2O_2) [Eq. (4)]. Then $^{\cdot}O_2{}^-$ and H_2O_2 inter-react to form hydroxyl radical $^{\cdot}OH$ [Eq. (5)]. Then, dye molecules are oxidized by these oxidants step by step [Eq. (6)]. In addition, the holes themselves can directly oxidize dye molecules (Rh B or MO), and this is considered as the dominant pathway, because it is the prerequisite step for the photo catalytic reaction that dye molecules adsorbed on the surface of CdS/TiO$_2$ [Eq. (7)] [22]. In this study, it is thought that both indirect oxidation by hydroxyl radical and direct oxidation by holes simultaneously functioned to oxidize dye molecules. By this token, the combination of CdS contributes to enhance photo catalytic efficiency under visible light irradiation owing to the photo-induced interfacial charge transfer.
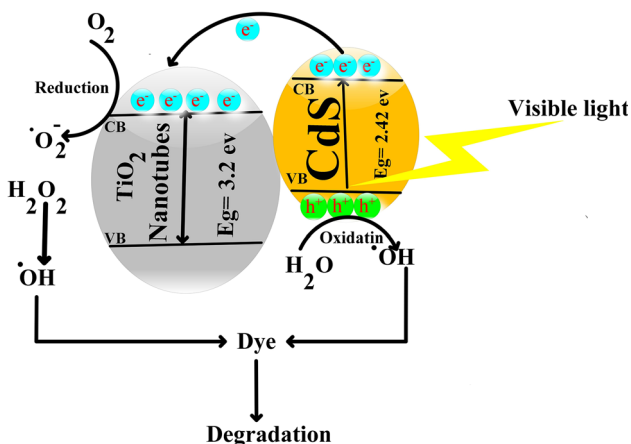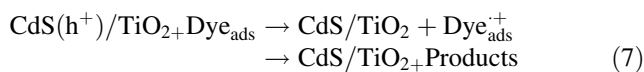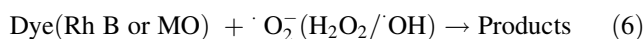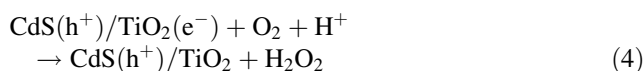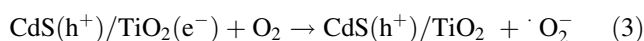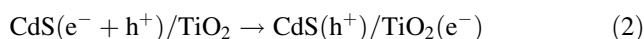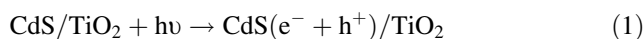
$$CdS/TiO_2 + h\upsilon \rightarrow CdS(e^- + h^+)/TiO_2 \tag{1}$$

$$CdS(e^- + h^+)/TiO_2 \rightarrow CdS(h^+)/TiO_2(e^-) \tag{2}$$

$$CdS(h^+)/TiO_2(e^-) + O_2 \rightarrow CdS(h^+)/TiO_2 + {}^{\cdot}O_2^- \tag{3}$$

$$\begin{aligned} &CdS(h^+)/TiO_2(e^-) + O_2 + H^+ \\ &\rightarrow CdS(h^+)/TiO_2 + H_2O_2 \end{aligned} \tag{4}$$

$$H_2O_2 + {}^{\cdot}O_2^- \rightarrow {}^{\cdot}OH + OH^- + O_2 \tag{5}$$

$$Dye(Rh\ B\ or\ MO) + {}^{\cdot}O_2^-(H_2O_2/{}^{\cdot}OH) \rightarrow Products \tag{6}$$

$$\begin{aligned} &CdS(h^+)/TiO_{2+}Dye_{ads} \rightarrow CdS/TiO_2 + Dye_{ads}^+ \\ &\rightarrow CdS/TiO_{2+}Products \end{aligned} \tag{7}$$

4 Conclusion

In summary, cadmium sulfide has been successfully deposited on titania nanotubes by successive ionic layer adsorption and reaction (SILAR) method for visible-light-driven organic compound degradation. The morphology, crystal structure, elemental composition and light absorption capability of samples were characterized by field emission scanning electron microscope, X-ray diffraction, energy dispersive X-ray spectrometer and ultraviolet–visible spectroscopy methods. Characterization of the cadmium sulfide–titania sample indicated that the number of

SILAR cycles significantly influenced the morphology and photo catalytic activity of fabricated films. Rhodamine B and methyl orange were adopted as the model dyes and the photo catalytic tests were carried out in detail. The activity of these samples through degradation of some dyes revealed that the photo catalytic activity of cadmium sulfide–titania samples is higher than that with bare titania sample. To further improve the photo catalytic efficiency on visible light region, some factors should be considered, including the light utilization efficiency, separation of the light-induced charge carries, large surface and strong interaction and structure matching between catalyst and contamination. The recyclability of CdS/TiO_2 samples showed that these samples have high stability and do not photo-corrode during this process. Such an important and useful property for these samples would greatly promote their practical application in a scale-up for industrial water remediation.

References

1. M.M. Momeni, Y. Ghayeb, Ceram. Int. **42**, 7014 (2016)
2. M.M. Momeni, Y. Ghayeb, J. Mater. Sci.: Mater. Electron. **27**, 1062 (2016)
3. M.M. Momeni, Y. Ghayeb, Solid. State Electrochem. **20**, 683 (2016)
4. M.M. Momeni, Y. Ghayeb, J. Iran. Chem. Soc. **13**, 481 (2016)
5. H. Tong, S. Ouyang, Y. Bi, N. Umezawa, M. Oshikiri, J. Ye, Adv. Mater. **224**, 229 (2012)
6. W. Zhao, Y. Sun, F.N. Castellano, J. Am. Chem. Soc. **130**, 12566 (2008)
7. M.M. Momeni, Z. Nazari, Ceram. Int. **42**, 8691 (2016)
8. R. Asahi, T. Morikawa, T. Ohwaki, K. Aoki, Y. Taga, Science **293**, 269 (2001)
9. S.U.M. Khan, M. Al-Shahry, W.B. Ingler, Science **297**, 2243 (2002)
10. K.P. Wang, H. Teng, Phys. Chem. Chem. Phys. **11**, 9489 (2009)
11. J. Liu, H. Yang, W. Tan, X. Zhou, Y. Lin, Electrochim. Acta **56**, 396 (2010)
12. M.M. Momeni, Y. Ghayeb, J. Mol. Catal. A: Chem. **417**, 107 (2016)
13. T. Ma, M. Akiyama, E. Abe, I. Imai, Nano Lett. **5**, 2543 (2005)
14. P. Hoyer, R. Konenkamp, Appl. Phys. Lett. **66**, 349 (1995)
15. X.F. Gao, H.B. Li, W.T. Sun, Q. Chen, F.Q. Tang, L.M. Peng, J. Phys. Chem. C **113**, 7531 (2009)
16. H. Lee, M. Wang, P. Chen, D.R. Gamelin, S.M. Zakeeruddin, M. Grätzel, M.K. Nazeeruddin, Nano Lett. **9**, 4221 (2009)
17. M.Y. Wang, L. Sun, J.H. Cai, P. Huang, Y.F. Su, C.J. Lin, J. Mater. Chem. A **1**, 12082 (2013)
18. M.Y. Wang, L. Sun, Z.Q. Lin, J.H. Cai, K.P. Xie, C.J. Lin, Energy Environ. Sci. **6**, 1211 (2013)
19. H.I. Okur, Y. Türker, O.M. Dag, Langmuir **26**, 538 (2009)
20. J.C. Kim, J. Choi, Y.B. Lee, J.H. Hong, J.I. Lee, J.W. Yang, W.I. Lee, N.H. Hur, Chem. Commun. **48**, 5024 (2006)
21. E.Y. Guo, L.W. Yin, L.Y. Zhang, CrystEngComm **16**, 3403 (2014)
22. L. Yu, D. Wang, D. Ye, Sep. Purif. Technol. **156**, 708 (2015)
23. C. Xue, T. Wang, G.D. Yang, B.L. Yang, S.J. Ding, J. Mater. Chem. A **2**, 7674 (2014)
24. J. Li, M.W.G. Hoffmann, H. Shen, C. Fabrega, J.D. Prades, T. Andreu, F.H. Ramirez, S. Mathur, J. Mater. Chem. **22**, 20472 (2012)
25. H. Wang, Y. Bai, H. Zhang, Z. Zhang, J. Li, L. Guo, J. Phys. Chem. C **114**, 16451 (2010)
26. J. Luo, L. Ma, T. He, C.F. Ng, S. Wang, H. Sun, H.J. Fan, J. Phys. Chem. C **116**, 11956 (2012)
27. C. Chen, G. Ali, S.H. Yoo, J.M. Kum, S.O. Cho, J. Mater. Chem. **21**, 16430 (2011)
28. W. Sun, Y. Yu, H. Pan, X. Gao, Q. Chen, L. Peng, J. Am. Chem. Soc. **130**, 1142 (2008)
29. C. Chi, Y. Lee, H. Weng, Nanotechnology **19**, 125704 (2008)
30. H.N. Hieu, N.Q. Dung, J. Kim, D. Kim, Nanoscale **5**, 5530 (2013)
31. X. Qi, G. She, Y. Liu, L. Mu, W. Shi, Chem. Commun. **48**, 242 (2012)
32. Y. Tak, S.J. Hong, J.S. Lee, K. Yong, J. Mater. Chem. **19**, 5945 (2009)
33. H.N. Hieu, N.M. Vuong, D. Kim, J. Electrochem. Soc. **160**, 852 (2013)
34. N.D. Quang, D. Kim, T.T. Hien, D. Kim, S.K. Hong, C. Kim, J. Electrochem. Soc. **163**, 434 (2016)
35. Y.F. Nicolau, Appl. Surf. Sci. **23**, 1061 (1985)
36. S. Lindroos, T. Kanniainen, M. Leskela, Appl. Surf. Sci. **75**, 70 (1994)